A&A 580, L6 (2015)
DOI: 10.1051/0004-6361/201526867

Astronomy & Astrophysics

Letter to the Editor

Radio emission from the Be/black hole binary MWC 656

S. A. Dzib, M. Massi, and F. Jaron

Max-Planck-Institut für Radioastronomie, Auf dem Hügel 69, 53121 Bonn, Germany
e-mail: [sdzib;mmassi;fjaron]@mpifr-bonn.mpg.de

Received 30 June 2015 / Accepted 15 July 2015

ABSTRACT

Context. MWC 656 is the recently discovered first binary system case composed of a Be-type star and an accreting black hole. Its low X-ray luminosity indicates that the system is in a quiescent X-ray state.

Aims. The aim of our investigation is to establish if the MWC 656 system has detectable radio emission and if the radio characteristics are consistent with those of quiescent black hole systems.

Methods. We used three archived VLA data sets, one hour each at 3 GHz, and seven new VLA observations, two hours each at 10 GHz, to produce very high sensitivity images down to ~1 μJy.

Results. We detected the source twice in the new observations: in the first VLA run, at apastron passage, with a flux density of 14.2 ± 2.9 μJy and by combining all together the other six VLA runs, with a flux density of 3.7 ± 1.4 μJy. The resulting combined map of the archived observations has the sensitivity of $1\sigma = 6.6$ μJy, but no radio emission is detected there.

Conclusions. The radio and X-ray luminosities agree with the behaviour of accreting binary black holes in the hard and quiescent state. In particular, MWC 656 in the L_X, L_R plane occupies the same region as A0620−00 and XTE J1118+480, the faintest known black holes up to now.

Key words. radio continuum: stars – X-rays: binaries – X-rays: individuals: MWC 656 – gamma rays: stars

1. Introduction

In 2010 the gamma-ray source AGL J2241+4454 was detected by the AGILE satellite (Lucarelli et al. 2010). Within the positional error circle of the satellite Williams et al. (2010) found the emission-line Be star MWC 656 (also known as HD 215227). The first suggested classification for MWC 656 was B3 IVne+sh, where *n* and *e* indicate broad lines and Balmer emission, and *sh* denotes the presence of shell lines, indicated by a sharp central absorption in the line. The V/R ratio of the Hγ emission changed significantly in one day, which is unusually fast for most Be stars and Williams et al. (2010) pointed out some resemblance of the spectral properties of this newly identified gamma-ray source to the gamma-ray binary LS I +61°303 and its Hα variations. The star MWC 656 is at a Galactic latitude of $b = -12°$; at a distance of $d = 2.6 \pm 0.6$ kpc the star results well below the Galactic plane at $z = -560 \pm 200$ pc. This is an extreme distance for a normal OB star and Williams et al. (2010) suggested a runaway star, which reached the current position by a supernova explosion of the companion star. Timing analysis of variations in the optical photometry, interpreted as orbital modulation, resulted in a period of 60.37 ± 0.04 days with the epoch of maximum brightness at HJD 2 453 243.3 ± 1.8.

The binary hypothesis was tested with a radial velocity study by Casares et al. (2012). Radial velocities folded with the 60.37 d of Williams et al. (2010) revealed a sine-like modulation. Casares et al. (2012) by the rotational broadening $v \sin i \sim 346$ km s^{-1} estimated the inclination of the orbit $i > 66°$ and a mass of the compact object in the range $M_c \sim 2.7$–5.5 $M_\odot$. Moreover, Casares et al. (2012) found that the main parameters of the Hα emission line (equivalent width, full width at half maximum, and centroid velocity) result to be modulated by the proposed orbital period.

The turning point in this research came with the new optical observations by Casares et al. (2014). To improve the radial velocity curve of the Be star, FeII emission lines from the innermost region of the Be disk were used instead of stellar broad absorption lines contaminated by the circumstellar wind emission lines. On the other hand, the spectra show an HeII 4686 Å double-peaked emission line, indicating a disk, whose centroid is modulated with the same 60.37 day period, but in antiphase with respect to the radial velocity of the Be star, as obtained from the FeII line (their Fig. 3). This important observation therefore hints at an accretion disk around an invisible companion. The orbital solution resulted in $\Phi_{\rm periastron} = 0.01 \pm 0.10$ (phase zero set to HJD 2 453 243.7). With new observations, the authors were also able to obtain a better spectral classification for the Be star, and determined a B1.5-B2 III classification. Given the mass of this star, 10–16 $M_\odot$, the implied companion mass is 3.8–6.9 $M_\odot$. This makes MWC 656 the first clear case of a Be-type star with a black hole companion. The case of LS I +61°303 is, in fact, still unclear because of the uncertainties in the values of mass function and inclination of the orbit (Massi 2004; Casares et al. 2005).

Observations with *XMM-Newton* at $\Phi = 0.08$ by Munar-Adrover et al. (2014) proved that MWC 656 is indeed an X-ray binary system. The X-ray luminosity of $\sim 10^{31}$ erg s^{-1} points to a stellar mass black hole in quiescence. The quiescent X-ray state is one of the X-ray states of an accreting black hole similar to the low-hard X-ray state. For a compact object of a few solar masses, the low/hard state corresponds to $L_X \sim 10^{36}$ erg s^{-1} but may drop to $L_X = 10^{30.5}$–$10^{33.5}$ erg s^{-1} (McClintock & Remillard 2006) at its lowest phase, called the quiescent state.

Table 1. MWC 656 observations and final parameters of maps.

Epoch	Date (day.month hh:mm)	Julian date	Φ	Synthesized beam ($\theta_{\rm maj}$ [″] × $\theta_{\rm min}$ [″]; PA [°])	rms noise (μJy beam^{-1})	Peak (μJy bm^{-1})	Flux ± σ^a (μJy)
X-band observations in 2015							
1	22.02 19:15	2457076.302	0.49	1.17 × 1.09; 101.7	2.9	9.9	14.2 ± 2.9
2	28.02 19:30	2457082.313	0.58	1.15 × 1.08; 104.3	3.8	...	<11.4
3	07.03 22:10	2457089.424	0.70	2.69 × 0.36; 58.8	2.3	...	<6.9
4	08.03 23:04	2457090.461	0.72	1.62 × 1.06; 84.6	2.4	...	<7.2
5	03.04 19:36	2457116.317	0.15	1.89 × 1.09; 89.3	2.2	...	<6.6
6	10.04 17:01	2457123.209	0.26	1.30 × 0.97; −20.6	2.7	...	<8.1
7	12.04 20:25	2457125.351	0.30	1.10 × 1.02; −21.9	2.3	...	<6.9
2–7				0.84 × 0.70; −75.1	1.02	3.47	3.7 ± 1.4
1–7				0.82 × 0.70; −75.1	0.95	4.15	4.5 ± 1.2
S-band observations in 2012							
1	05.10 04:38	2456205.693	0.06	0.48 × 0.41; 12.3	12.6	...	<37.8
2	15.10 08:03	2456215.835	0.23	0.66 × 0.44; 89.6	10.1	...	<30.3
3	06.12 04:54	2456267.704	0.09	0.61 × 0.50; 83.0	11.1	...	<33.3
1–3				0.51 × 0.45; 80.5	6.6	...	<19.8

Notes. [(a)] Upper limits at three times the noise level.

The X-ray luminosity in the quiescent and low/hard X-ray states correspond to a radiatively inefficient, "jet-dominated" accretion mode (Fender et al. 2003). In this mode, only a negligible fraction of the binding energy of the accreting gas is directly converted into radiation. Most of the accretion power emerges in kinetic form, as shown for Cygnus X-1 by Gallo et al. (2005), and for AGNs through the relationship between the Bondi power and the kinetic luminosity (Merloni & Heinz 2007, and references therein). That is, during the low-hard and quiescent states the liberated energy of the accretion is thought to be converted into magnetic energy, which powers the relativistic jet observed in these states (Gallo et al. 2003; Gallo et al. 2006; Fender et al. 2004; Smith 2012).

The origin of the X-ray emission during the low-hard and quiescent states is still controversial. The emission may be due to a Comptonizing corona and/or to the jet (see Gallo et al. 2006). Nevertheless, it is well established that the X-ray emission is related to the radio emission from the jet (Gallo et al. 2003; Gallo et al. 2006; Merloni et al. 2003). This important nonlinear scaling between X-ray and radio luminosities, $L_{\rm X}$, $L_{\rm R}$, has been demonstrated to hold, with the addition of a mass term, across the entire black hole mass spectrum, from microquasars to AGN (Merloni et al. 2003).

Therefore, if a jet is associated with MWC 656, its radio emission should be consistent with the $L_{\rm X}$, $L_{\rm R}$ relationship. The aim of our investigation is to establish if the system MWC 656 has an associated radio emission and if the radio emission fulfills the $L_{\rm X}$, $L_{\rm R}$ relationship. In this letter, we present new radio observations in the direction of this system. Section 2 describes the observations and the data reduction. In Sect. 3 we report on our results. Section 4 describes MWC 656 in the context of the $L_{\rm X}$, $L_{\rm R}$ relationship, and finally, Sect. 5 gives our conclusions.

2. Observations

We obtained seven new *X*-band (8 to 12 GHz) observations with the Karl G. Jansky Very Large Array (VLA) of the National Radio Astronomy Observatory (NRAO) in its B configuration. These observations were made under project 15A-013. The receiver was used in semicontinuum mode with the 3 bit sampler and 32 different spectral windows (with bandwidths of 125 MHz) were recorded simultaneously to cover the full band.

Each observing session ran for two hours and was organized as follows. First, we spent 4.5 min on scans for instrument setups as recommended by NRAO[1]. Then, we observed a 5.5 min scan on the phase calibrator J2255+4202, and the large scan was performed to take the slewing time into account. Then we observed nine cycles of 10.6 min on the target followed by 1.0 min on the phase calibrator. We finished the observation with a 5.5 min scan in the flux calibrator 3C 147, which was also used as the bandpass calibrator. We spent ~95 min on target per epoch, or a total of ~668 min.

The data were edited and calibrated using the Common Astronomy Software Applications (CASA 4.2.2) package, and the VLA calibration pipeline in its 1.3.1 version. After calibration images were produced with pixel sizes of 0.2 arcsec, a natural weighting, and a multifrequency synthesis scheme (e.g., Rau & Cornwell 2011). The noise levels reached for each individual observation was about ~3 μJy (see Table 1). Additionally, we produced images from the concatenated UV data from the epoch 2 to 7 and of the seven observations to reach lower noise levels of 1.02 μJy and 0.95 μJy, respectively. These noise levels are in agreement with the theoretically expected values.

Finally, we also performed the data reduction of three archived *S*-band (2–4 GHz) data sets taken with the VLA in its A configuration; these are part of the project 12B-061. Each individual epoch runs for 1.0 h. The receiver was also used in semicontinuum mode with the 8 bit sampler and 16 different spectral windows (with bandwidths of 125 MHz each) were recorded simultaneously to cover the full band. These observations used the quasar 3C 48 as the flux and bandpass calibrator, and quasar J2202+4216 as the phase calibrator.

The data were edited, calibrated, and imaged following the same scheme as the new observations. The resulting sensitivity limits are ~11 μJy and 6.6 μJy, for the maps of individual epochs and for the map of the concatenated epochs (see also Table 1),

[1] https://science.nrao.edu/facilities/vla/docs/manuals/obsguide

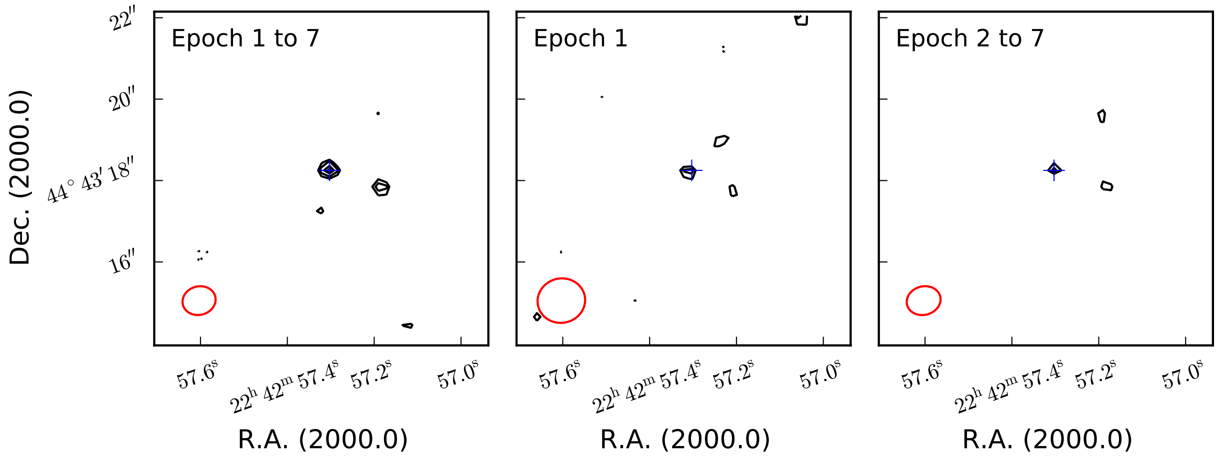

Fig. 1. VLA images with radio emission at the MWC 656 position. *Left*: concatenated *X*-band data from Epoch 1 to 7. *Center*: Epoch 1. *Right*: concatenated *X*-band data from Epoch 2 to 6. Contour levels are −3, 2.8, 3.2, 3.8, and 4.2 times the noise levels of the image (see Table 1). The red ellipse at the bottom left is the corresponding synthesized beam. The blue cross indicates the optical position of MWC 656.

respectively. These values are also in agreement with those theoretically expected.

3. Results

A source with a peak 3.4 times the noise level was detected in the first observation at orbital phase $\Phi = 0.49$, i.e., at apastron passage. The source is coincident with the position of MWC 656 (see Fig. 1, center). A Gaussian fit to the source (using *imfit* in CASA) yields the flux density of the source to be 14.2 ± 2.9 μJy. In the remaining observations, however, we do not detect any peak above 2.6 times the noise level of the images (see Fig. 2). By adding these six remaining observations, we detected a source with a peak 3.4 times the noise level, which is coincident in position with MWC 656 and with the source detected in the first epoch (see Fig. 1, right). The flux density in this case was 3.7 ± 1.4 μJy. The two images of Fig. 1 (center, right) were produced with independent data sets, and support our detection of the radio counterpart of MWC 656. Interestingly, the flux in the first image (Fig. 1, center) has a flux density almost three times higher than that in Fig. 1, right, and this increased flux is occurring at apastron. We produce a final map by concatenating the data of the seven observed epochs. The source is now detected at levels of 4.4 times the noise in the image (Fig. 1, left). The Gaussian fit to the source yields the flux density of the source to be 4.5 ± 1.2 μJy, at the position $\mathrm{RA} = 22^{\mathrm{h}}42^{\mathrm{m}}57\overset{\mathrm{s}}{.}305 \pm 0\overset{\mathrm{s}}{.}005$, $\mathrm{Dec} = +44°43'18\overset{''}{.}23 \pm 0\overset{''}{.}08$, and is consistent with a point like structure and parameters of Table 1. The source position is in good agreement with the optical position of MWC 656, $\mathrm{RA} = 22^{\mathrm{h}}42^{\mathrm{m}}57\overset{\mathrm{s}}{.}30295$, $\mathrm{Dec} = +44°43'18\overset{''}{.}2525$ (van Leeuwen 2007).

Finally, concerning the archived data (Table 1), we did not detect the source in any single *S*-band epoch, nor in the final image of concatenated observations at levels above 20 μJy.

4. MWC 656 in the context of the L_{X}, L_{R} relationship

The radio flux values of 3.7 ± 1.4 μJy and 14.2 ± 2.9 μJy at 10 GHz, for a distance of 2.6 kpc, and assuming a nearly flat spectrum, corresponds to a L_{R} at 8.6 GHz of 2.6×10^{26} erg s^{-1} and 9.9×10^{26} erg s^{-1}, respectively. Munar-Adrover et al. (2014) determined an X-ray luminosity of $L_{\mathrm{X}} = 1.2 \times 10^{31}$ erg s^{-1} from an observation at $\Phi = 0.08$. We report our new data of MWC 656 along with the measurements from Corbel et al. (2013). Figure 3 shows (square/black) the radio and X-ray luminosities for the 24 Galactic accreting binary BHs in the hard and quiescence states reported in Fig. 9 of Corbel et al. (2013). The position of MWC 656, given in red color, is rather close to the position of

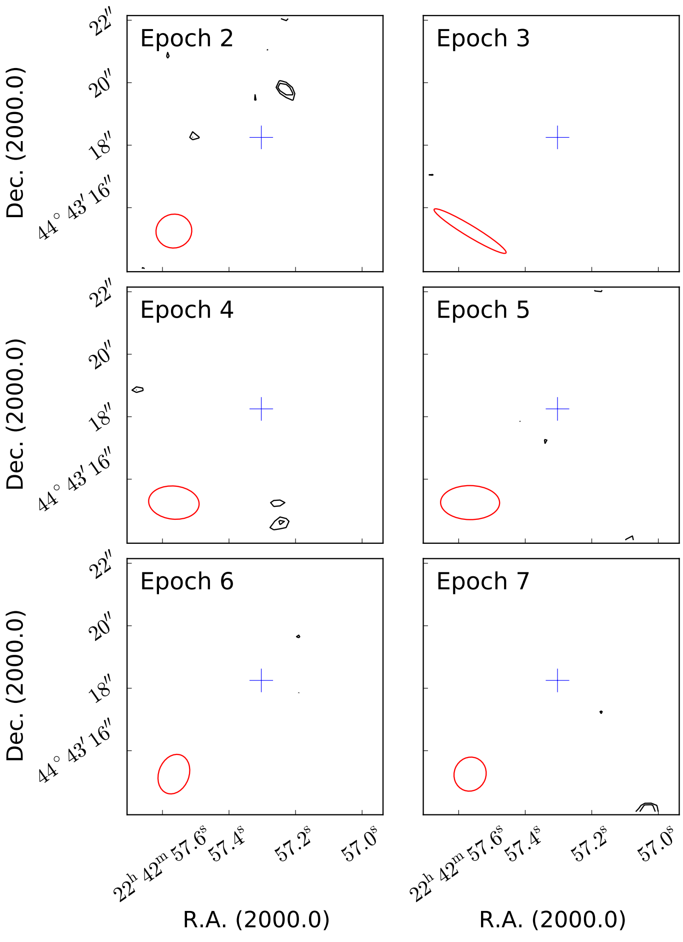

Fig. 2. VLA images from epoch 2 to 7. The red circle at bottom-left is the synthesized primary beam. Contours are at −3, 2.6, and 3 times the noise level. The blue cross at the center represents the position of MWC 656. The source remains undetected in each single image. The rms of the images and upper limits for the flux density of MWC 656 are given in Table 1.

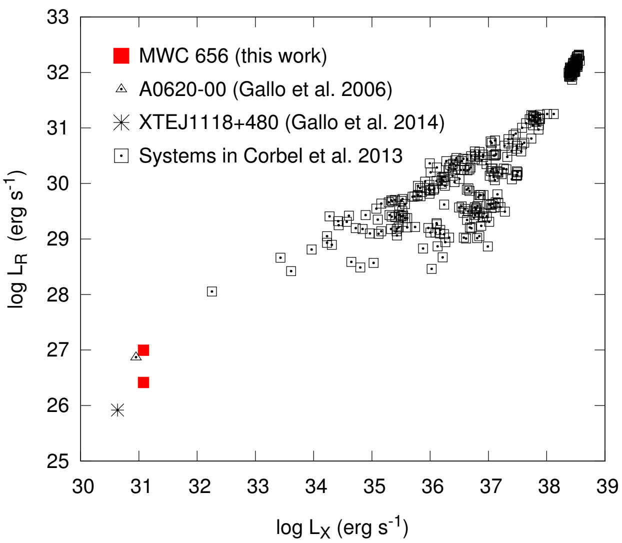

Fig. 3. Radio (8.6 GHz) vs. X-ray luminosity (1–10 keV) diagram. Black squares indicate the positions of the 24 Galactic accreting binary black holes in the hard and quiescence states, as in Fig. 9 of Corbel et al. (2013; i.e., without the upper limits and neutron stars there present). The position of MWC 656 is indicated by two red squares for the two fluxes of 3.7 μJy and 14.2 μJy. The position of MWC 656 is rather close to the faintest accreting black hole systems known so far, A0620-00 (triangle, Gallo et al. 2006) and XTE J1118+480 (asterisk, Gallo et al. 2014).

A062000 and XTE J1118+480, which are the weakest quiescent black holes known so far (Gallo et al. 2006; Gallo et al. 2014).

5. Conclusions

Deep VLA observations of the BH-Be system MWC 656 have provided us with the first radio detection of an accreting stellar mass black hole with a Be star as companion. Along with a level of emission of 3.7 ± 1.4 μJy, determined combining six observations at the different orbital phases Φ = 0.58–0.72 and Φ = 0.15–0.30, we detected in a single observation around apastron (Φ = 0.49) the flux density of 14.2 ± 2.9 μJy.

Several works have placed significant constrains on the L_X–L_R luminosities of quiescent systems (e.g., Gallo et al. 2006; Gallo et al. 2014; Calvelo et al. 2010; Miller-Jones et al. 2011). The nonsimultaneous *XMM-Newton* X-ray observation by Munar-Adrover et al. (2014) at orbital phase Φ = 0.08, also allowed us to test for MWC 656 the X-ray/radio correlation for black holes. The position of MWC 656 is close to the faintest black holes known so far, which are A0620-00 and XTE J1118+480. The secondary star in A0620–00 is a 0.7 $M_{\odot}$ K3–K4V star in a 7.75 h orbit around the black hole (Gallo et al. 2006). The companion star in XTE J1118+480 is a K5–K8V star with an orbital period of 4.08 h (Gallo et al. 2014, and references therein). MWC 656 has an orbit of ~60 days and the companion star is a 10–16 $M_{\odot}$ Be star. Our observations support, therefore, the universality of the L_X, L_R relationship, which is intimately related to the accretion-ejection coupling process, which seems to be invariant to different forms of accretion.

Acknowledgements. We acknowledge Pere Munar-Adrover, Luis F. Rodríguez and Alberto Sanna for comments and suggestions in the manuscript. The data set of Fig. 3 is provided by S. Corbel with support from the Agence National de la Recherche for the CHAOS project. The National Radio Astronomy Observatory is operated by Associated Universities Inc. under cooperative agreement with the National Science Foundation.

References

Calvelo, D. E., Fender, R. P., Russell, D. M., et al. 2010, MNRAS, 409, 839
Casares, J., Ribas, I., Paredes, J. M., Martí, J., & Allende Prieto, C. 2005, MNRAS, 360, 1105
Casares, J., Ribó, M., Ribas, I., et al. 2012, MNRAS, 421, 1103
Casares, J., Negueruela, I., Ribo, M., et al. 2014, Nature, 505, 378
Corbel, S., Coriat, M., Brocksopp, C., et al. 2013, MNRAS, 428, 2500
Fender, R. P., Gallo, E., & Jonker, P. G. 2003, MNRAS, 343, L99
Fender, R. P., Belloni, T. M., & Gallo, E. 2004, MNRAS, 355, 1105
Gallo, E., Fender, R. P., & Pooley, G. G. 2003, MNRAS, 344, 60
Gallo, E., Fender, R. P., & Hynes, R. I. 2005, MNRAS, 356, 1017
Gallo, E., Fender, R. P., Miller-Jones, J. C. A., et al. 2006, MNRAS, 370, 1351
Gallo, E., Miller-Jones, J. C. A., Russell, D. M., et al. 2014, MNRAS, 445, 290
Lucarelli, F., Verrecchia, F., Striani, E., et al. 2010, The Astronomer's Telegram, 2761, 1
Massi, M. 2004, A&A, 422, 267
McClintock, J. E., & Remillard, R. A. 2006, Compact stellar X-ray sources (Cambridge University Press), 157
Merloni, A., & Heinz, S. 2007, MNRAS, 381, 589
Merloni, A., Heinz, S., & di Matteo, T. 2003, MNRAS, 345, 1057
Miller-Jones, J. C. A., Jonker, P. G., Maccarone, T. J., Nelemans, G., & Calvelo, D. E. 2011, ApJ, 739, L18
Munar-Adrover, P., Paredes, J. M., Ribó, M., et al. 2014, ApJ, 786, L11
Rau, U., & Cornwell, T. J. 2011, A&A, 532, A71
Smith, M. D. 2012, Astrophysical Jets and Beams (Cambridge University Press)
van Leeuwen, F. 2007, A&A, 474, 653
Williams, S. J., Gies, D. R., Matson, R. A., et al. 2010, ApJ, 723, L93